Available online at http://ijcpe.uobaghdad.edu.iq and www.iasj.net
Iraqi Journal of Chemical and Petroleum Engineering
Vol. 24 No. 4 (December 2023) 115 – 125
EISSN: 2618-0707, PISSN: 1997-4884

Anodic and Cathodic preparation of MnO_2/Co_2O_3 Composite Electrode Anodes for Electro-Oxidation of Phenol

Yamama A. Ahmed [a], Rasha H. Salman [a], Fatma Kandemirli [b, *]

a Department of Chemical Engineering, College of Engineering, University of Baghdad, Baghdad, Iraq
b Kastamonu University, Faculty of Engineering and Architecture, Biomedical Engineering Department, 37150, Kastamonu, Türkiye

Abstract

The economical and highly performed anode material is the critical factor affecting the efficiency of electro-oxidation toward organics. The present study aimed to detect the best conditions to prepare Mn-Co oxide composite anode for the electro-oxidation of phenol. Deposition of Mn-Co oxide onto graphite substrate was investigated at 25, 30, and 35 mA/cm^2 to detect the best conditions for deposition. The structure and the crystal size of the Mn-Co oxide composite electrode were examined by using an X-Ray diffractometer (XRD), the morphological properties of the prepared electrode were studied by scanning electron microscopy (SEM) and Atomic force microscopy (AFM) techniques, and the chemical composition of the various deposited oxide was characterized by energy dispersive X-ray spectroscopy (EDX). The study also highlighted the effect of current density (40, 60, and 80 mA/cm^2), pH (3, 4, and 5), and the concentration of NaCl (1, 1.5, and 2 g/l) on the anodic electro-oxidation of phenol was investigated. The results revealed that the composite anodes are successfully prepared galvanostatically by anodic and cathodic deposition. In addition, the current density of 25 mA/cm^2 gave the best cathodic deposition performance. The removal efficiency of phenol and other by-products increased as the current density and the concentration of NaCl in the electrolyte increased, while it decreased as the pH increased. The prepared composite electrode gave high COD removal efficiency (98.769 %) at the current density of 80 mA/cm^2, pH= 3, NaCl conc. of 2 g/L within 3 h.

Keywords: manganese oxide, cobalt oxide, phenol, composite electrode, electrodeposition, electro-oxidation.

Received on 03/03/2023, Received in Revised Form on 16/04/2023, Accepted on 16/04/2023, Published on 30/12/2023

https://doi.org/10.31699/IJCPE.2023.4.12

1- Introduction

Globally, there is an increasing need for petroleum products, which increases the risks to the environment. One of these problems is caused by the large amounts of wastewater produced during the process of refining crude oil, which includes a variety of contaminants in the range of 0.6 to 1.4 tons of wastewater produced for every ton of oil produced [1 - 3]. Phenol and its derivatives are among the most frequent organic contaminants found in the industrial wastewater from the oil refining industry. They are also found in the waste products of other industries including petrochemicals, pharmaceuticals, coking processes, resin manufacture, plastics, paint, pulp, paper, textiles, wood products pesticides, and herbicides [4 - 8]. Due to their high toxicity, limited biodegradability, and severe effects on the environment, people, and animals; these chemicals are particularly dangerous even in small amounts. Phenol poses serious health risks to people since it is a possible human carcinogen. According to the Protection Agency, phenol is one of the most dangerous toxins and should be rapidly eliminated from all waste streams. The wastewater discharge standards for phenol are set at 0.005 mg/L for groundwater and 0.05 mg/L for the sewage treatment plant [9, 10].

Adsorption, biological treatment, chemical oxidation, distillation, precipitation, ion exchange, solvent extraction, reverse osmosis, membrane processes, electro-oxidation, and electrocoagulation are some technologies that have been utilized to remove phenol from aqueous solutions [11 - 15]. Because electrons are a versatile, effective, clean reagent, easily automatable, and possess a higher pollutant degrading efficiency than standard techniques, electrochemical technologies provide an alternative solution to many environmental issues in the process industry [16 - 19].

Electrochemical technologies provide an alternative solution to many environmental issues in the process industry because electrons are versatile, effective, clean reagents, easily automatable, and possess a higher pollutant degrading efficiency than standard techniques [16 - 23].

Both direct and indirect anodic oxidation can be utilized in the electrochemical process to degrade organic contaminants. In direct anodic oxidation, pollutants are first bound onto the anode surface before being removed by the anodic electron transmission reaction. At the anode, chloride ions combine with electrons to form active chlorine species such as hypochlorous acid (HOCl),

*Corresponding Author: Name: Fatma Kandemirli, Email: fkandemirli@kastamonu.edu.tr

chlorine, and hypochlorite ions, which attack organic molecules and break them down into harmless byproducts. Hypochlorous acid is a very strong oxidant that is produced in the bulk solution at an acidic medium, and it is more reactive than the hypochlorite ion, after that, the pollutants in the whole solution are flushed out. [12, 24- 26].

Numerous variables, including electrode material, current density, and the existence of species in the solution that can act as mediators, flow dynamic regime, and pH influence the effectiveness of an electrochemical process [28- 30].

When choosing electrodes for electro-oxidation of organic and inorganic pollutants, several factors need to be considered. These include the stability, selectivity, expenses, and ecological impact of the electrode material, as well as the content and characteristics of the wastewater that will be treated [31].

Electrodeposition is an effective technique in preparing composite substrates for electrochemical applications since it directly deposits oxide layers on a substrate surface and has been used successfully to produce electrolytic metal oxides. Additionally, the process only requires one step; it is straightforward and inexpensive in terms of equipment, allows for perfect control of the thickness of the deposit, is template-free, clean, and economical, appropriate for large-scale applications, and is easily controlled [32, 33].

The goal of this work is the electrodeposition of the composite metal electrodes galvanostatically onto graphite from cobalt nitrate and manganese chloride solution with different current densities (25, 30, and 35 mA/cm^2). Binary composite electrodes had been studied for supercapacitors and very few previous studies investigated the removal of phenol by binary composite electrodes. Therefore, in the present study, utilizing the composite electrode during the electro-oxidation of phenol has been examined with different conditions (current density, pH, and NaCl) to detect the beat conditions for indirect oxidation of phenol.

2- Experimental Work

2.1 Electrodeposition Process

Composite Electrodes (manganese oxide and cobalt oxide) were prepared by electrodeposition process. The cell was made up of two graphite electrodes with dimensions (12 cm*5 cm*1 cm) fixed in a glass electrolytic bath. To improve particle adherence to graphite, the graphite electrodes were heated to 350°C for 30 minutes in a furnace [34]. After that, they were cleaned with distilled water. The graphite electrodes were prepared with distilled water after being cleaned with acetone to eliminate surface contaminants and the oxide layer before every experiment.

The electrolytic solution for deposition was prepared from 0.2 M of $MnCl_2{\cdot}4H_2O$ and 0.2M of $Co(NO_3)_2{\cdot}6H_2O$ with a ratio (1:1) dissolved in 600 ml of distilled water. The specification of materials is mentioned in our previous study [35]. Graphite electrodes were placed vertically (with an active area of 25 cm^2) in the electrolyte bath with a distance of 3 cm between electrodes, and they connected to (DC) power supply (MS-605D, China) as shown in Fig. 1. The deposited film of manganese and cobalt oxide onto the anode and the cathode of graphite electrodes were investigated by applying various direct current densities (25, 30, and 35 mA/cm^2) for 2 h. After deposition, the graphite electrodes were washed with distilled water. The green and brownish/gold colors of deposited graphite indicated the existence of manganese and cobalt oxides, respectively [36].

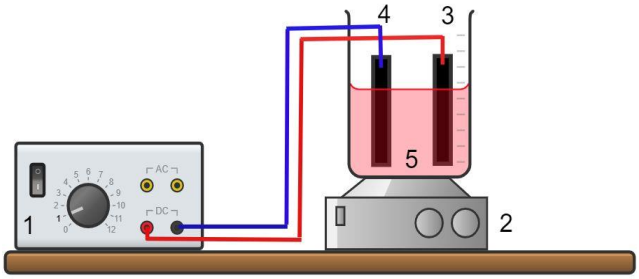

Fig. 1. The Electrochemical Cell Schematic (1. DC power supply, 2. Magnetic stirrer, 3. Graphite anode 4. Graphite cathode 5. beaker)

2.2 Phenol Electro-Oxidation Process

Each prepared metal oxide composite electrode (anode or cathode) was utilized as an anode in the system of electro-oxidation of phenol, while graphite was utilized as the cathode. The performance of the synthesized electrodes was detected by adopting them as anodes to remove phenol from an aqueous solution with 150 mg/l of phenol (equivalent to 320 mg/l of COD) using 0.1 M of H_2SO_4 and a specified quantity of NaCl as the supporting electrolyte. For the phenol removal studies, a volume of 600 ml was used, and a temperature of about 25 ±1°C was maintained throughout the experiments. The electrochemical removal experiments were took place under the specified operating parameters: current densities of 40, 60, and 80 mA/cm^2; NaCl conc. of 1, 1.5, and 2 g/L, an initial phenol concentration of 150 mg/l; an electrolysis time up to 3 h, and a pH of 3, 4, and 5. Each experiment was duplicated, and the average value of COD was taken, and the COD would be utilized to detect the accurate value of removal for phenol and any other organic by-products that may be produced during the indirect oxidation process [29]. Eq. 1 shows the COD removal efficiency.

$$COD\ Removal\% = \frac{COD_o - COD_f}{COD_o} \times 100 \quad (1)$$

Where: COD_o and COD_f are both the initial and final values of COD, respectively.

The samples were taken at the beginning and the end of the electrolysis process and subjected to the established colorimetric method by (Lovibond water testing, Photometer- System MD200) for COD characterization [29].

3- Results and Discussion

3.1. XRD analysis

To detect the crystal structure of the prepared electrodes which were prepared with different current densities (25, 30, and 35 mA/cm^2). Fig. 2 to Fig. 4 show the XRD spectra of the deposited anode and cathode electrodes. A1, B1, and C1 referenced the anode electrode, while A2, B2, and C2 referenced the appropriate cathode electrode, where A, B, and C represented 25, 30, and 35 mA/cm^2, respectively.

The XRD spectra show diffraction peaks in all prepared electrodes at 2θ=31.83° (220), 37.4° (311), and 65.33° (440) which are associated with the cubic phase of Co_3O_4 and the observed '*d*' values match with standard '*d*' values are taken from JCPDS card no-042-1467. However, XRD spectra also show the diffraction peaks at 2θ= 28.09°, 36.5°, 41.8°, and 60.06° which are associated with (310), (211), (301), and (521) planes. These peaks are associated with orthorhombic MnO_2 and hexagonal MnO_2 that match with JCPDS card No.044-1316 and No.030-0820, respectively.

The XRD pattern also indicates the presence of a cubic spinel structure of $MnCo_2O_4$. These peaks corresponding to 18.79°, 31.27°, 34.62°, 37.10°, 38.72°, 45.04°, 55.57°, 59.46°, 65.13°, 77.61°, and 78.26° can be indexed to crystal planes of (111), (220), (311), (222), (400), (422), (511), (531), (533), and (622). The values are in agreement with JCPDS database number 023-1237.

Many peaks in the XRD patterns seemed weak and broad, which indicates the samples' low crystallinity. Low lattice energy, which is related to poor crystallinity, is useful for electrode materials because it makes the deintercalation process simpler [36]. The XRD patterns of the prepared electrodes show noticeable variation, and all of the strong diffraction peaks are related to the graphite substrates. The deposited oxide merely added a wider peak with a very low intensity near 37° in each pattern; it should be emphasized. A previous study by [38] provided evidence that the binary Mn-Co oxides and plain Mn oxide were both nanocrystalline materials. In other words, the crystal structure of the pure Mn oxide did not appear to be impacted by the incorporation of Co oxide.

3.2. SEM analysis

The morphology of prepared deposited electrodes was observed by SEM. The anode materials' morphology differed from the cathode materials' as shown in Fig. 5 to Fig. 7 which illustrate SEM images at different magnifications with different current densities (25, 30, and 35 mA/cm^2). Generally, the anode materials were regarded as blocks with powders. Due to the low conductivity of metal oxides, the oxidation reaction occurred preferentially at the thinner parts of the film, filling the pocket to make the film flat. This structure suggests that oxidation and deposition of metal ions could occur simultaneously on the electrode. The surface area of the anode materials is expected to be low [39].

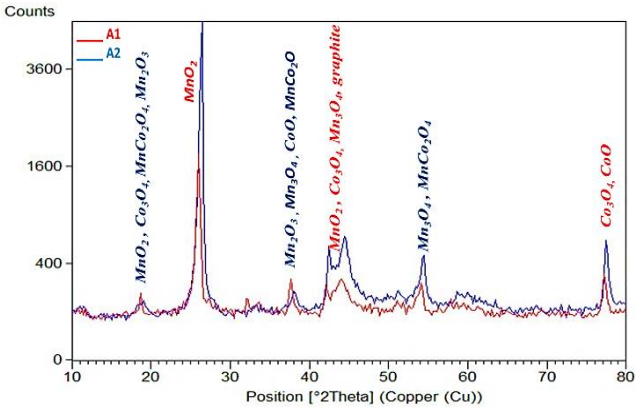

Fig. 2. XRD Analysis of Co-Mn Oxide (0.2- 0.2 M) for Anode (A1), and Cathode (A2) at Current Density = 25 mA/cm^2

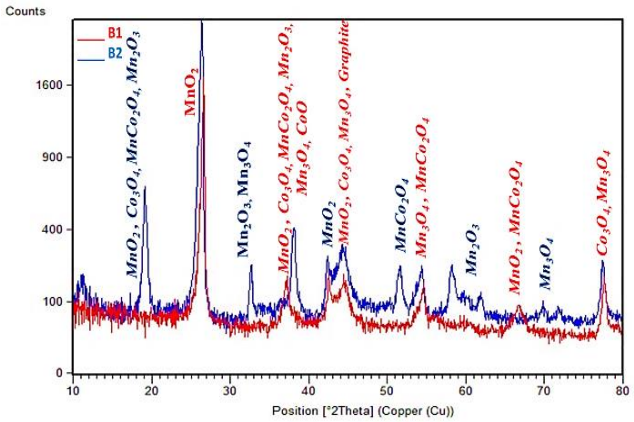

Fig. 3. XRD Analysis of Co-Mn Oxide (0.2- 0.2M) for Anode (B1), and Cathode (B2) at Current Density = 30mA/cm^2

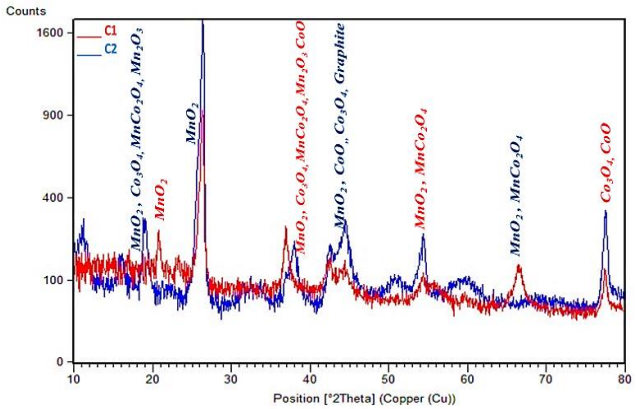

Fig. 4. XRD Analysis of Co-Mn Oxide (0.2- 0.2M) for Anode (C1), and Cathode (C2) Current Density = 35 mA/cm^2

The cathode substrates at 25 mA/cm^2 were well covered with nanofibers metal oxides. Porous spaces were observed between the nanofibers, enhancing the redox process as confirmed in the previous study by[40]. It is well known that the energy available for creating new grain nuclei is affected by the cathodic overpotential. When the current density is modest (about 25 mA/cm^2), a coarse-grained structure forms because the grain growth rate exceeds the nuclei formation rate. When the current density is raised to 30 mA/cm2, the overpotential increases, and the granules smooth out. As can be seen in Fig. 6B1 and Fig. 6B2, the grains have reduced and transformed into spherical shapes. The embedded particles are also more concentrated and uniformly dispersed. SEM photos reveal a decent degree of surface covering, however as the current density is increased to 35 mA/cm^2, peeling is detected on the surface of the composite coating, which is consistent with prior research [29, 41, 42]. As the current density increases from 25 mA/cm^2 up to 35 mA/cm^2, the amount of Co_3O_4 particles slightly decreases, and the amount of MnO_2 particles in the coating increases gradually [43, 44].

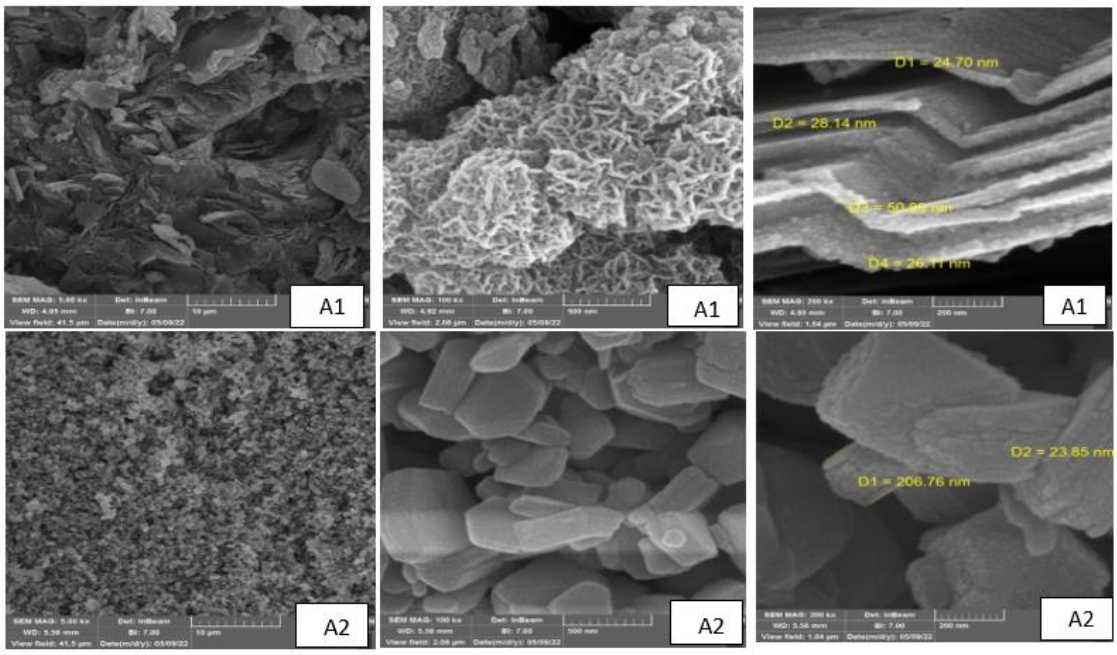

Fig. 5. SEM of Co-Mn Oxides (0.2- 0.2 M) of Anode (A1), and Cathode (A2) at Current Density 25mA/cm^2 and at Different Magnification (5kx, 100kx, and 200 kx, respectively)

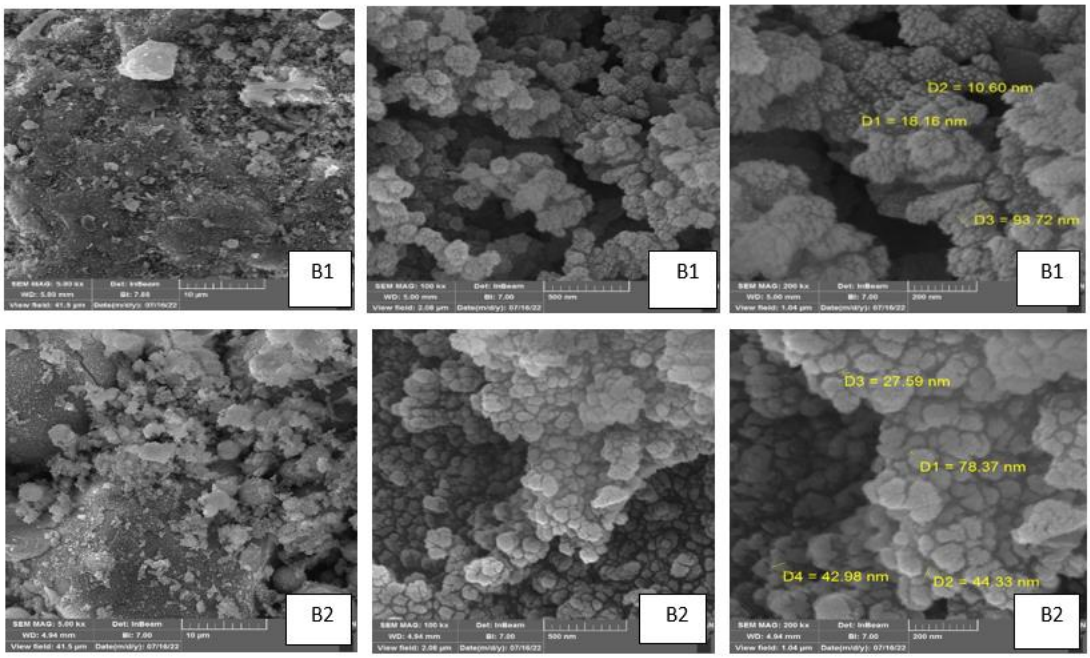

Fig. 6. SEM of Co-Mn Oxides (0.2- 0.2 M) of Anode (B1), and Cathode (B2) at Current Density 30mA/cm^2 and at Different Magnification (5kx, 100kx, and 200 kx, respectively)

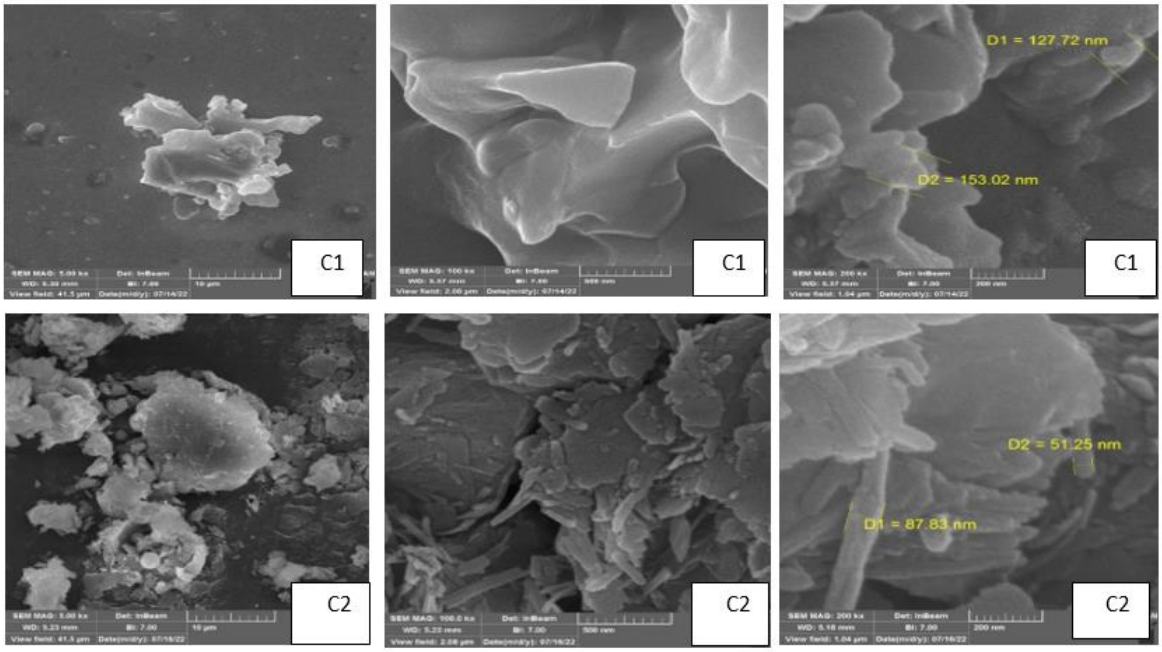

Fig. 7. SEM of Co-Mn Oxides (0.2- 0.2 M) of Anode (C1), and Cathode (C2) at Current Density 35mA/cm^2 and at Different Magnification (5kx, 100kx, and 200 kx, respectively)

3.3. EDX analysis

The elemental compositions of the prepared cathodes and the anodes of Mn-Co composites at various current densities were tested using EDX. The EDX spectra showed the presence of Co, Mn, and O. It is shown that increasing current density leads to a slight difference in the amount of Co and Mn as illustrated in Table 1.

Table 1. EDX Spectra of Anode and Cathode of Mn-Co Oxides at Various Current Densities (25, 30, and 35 mA/cm^2)

	Anode		Cathode	
		25 mA/cm^2		
Element	**Wt.%**	**At. %**	**Wt.%**	**At. %**
O	53.38	79.74	51.84	79.97
Mn	19.24	8.53	18.26	8.06
Co	27.39	11.73	29.90	12.89
Sum	100.00	100.00	100.00	100.00
		30 mA/cm^2		
Element	**Wt.%**	**At. %**	**Wt.%**	**At. %**
O	52.38	79.74	52.84	80.05
Mn	19.24	8.53	18.27	8.06
Co	28.39	11.73	28.90	11.89
Sum	100.00	100.00	100.00	100.00
		35 mA/cm^2		
Element	**Wt.%**	**At. %**	**Wt.%**	**At. %**
O	53.09	80.19	50.72	78.62
Mn	19.17	8.43	20.75	9.37
Co	27.74	11.38	28.53	12.01
Sum	100.00	100.00	100.00	100.00

3.4. AFM analysis

Fig. 8 (A1 to C1) shows the AFM images of anodes' surfaces which are deposited under the various current densities, it is clear that the roughness (root mean square, RMS) of the Co-Mn oxide deposit decreased with increasing current density hence small deposits and rapid nucleation occur at a high applied current during the electrodeposition process, other authors had verified this finding [45].

AFM pictures of the surfaces of cathodes prepared at various current densities are shown in Fig. 8 (A2 to C2). The number of deposition sites reduces and the surface becomes rougher as the current density rises from 25 mA/cm^2 to 35 mA/cm^2, and those results agree with previous studies [29, 46, 47]. According to the higher measured RMS (as shown in Table 2) of the surface roughness, the metal oxide deposition on the cathode is rougher than the metal oxide deposition on the anode due to the hydrogen evolution at the cathode that increased as current density increases [47].

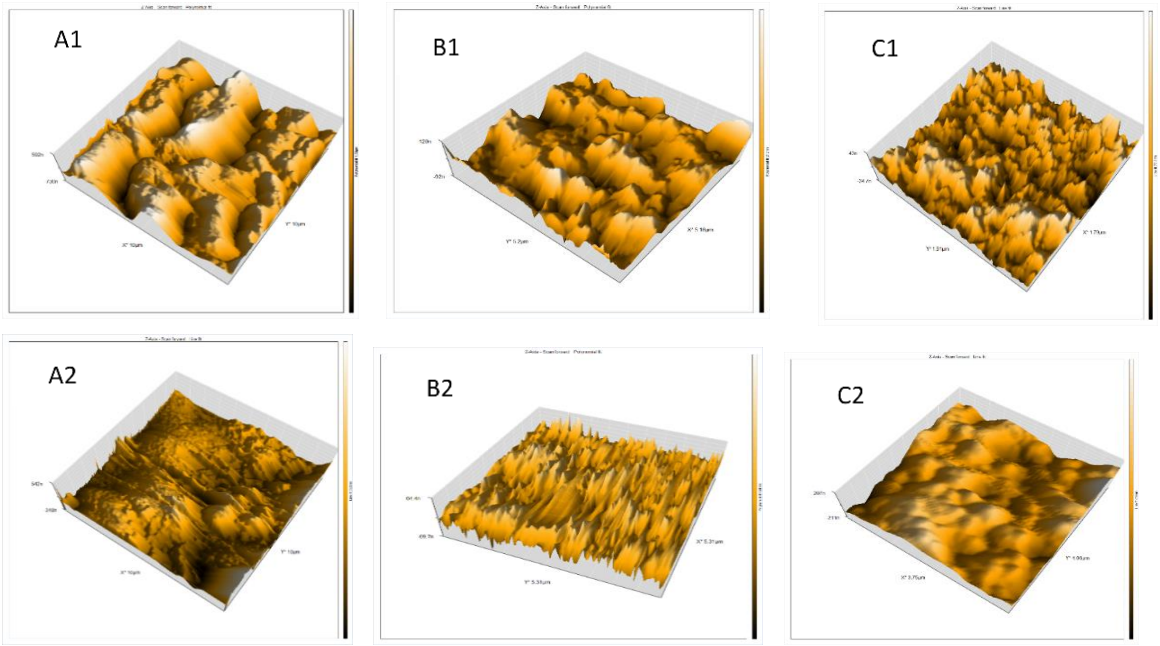

Fig. 8. AFM Images for Co-Mn Oxide (0.2-0.2 M) Anode (A1, B1, and C1), and Cathode (A2, B2, and C2) at Various Current Densities (25, 30, and 35 mA/cm^2)

Table 2. Root Mean Square (nm) of Anode and Cathode of Mn-Co Oxides at Different Current Densities

Current density mA/cm^2	Root mean square, nm	
	Anode	Cathode
25	28.33	37.78
30	14.4	46.8
35	10.68	48.33

3.5. Phenol Removal

The performance of the prepared composite anode and cathode was studied by anodic electro-oxidation of phenol with an initial conc. of 150 mg/l that is equivalent to COD of 320 mg/l in the presence of a different concentration of NaCl and 0.1 M H_2SO_4 to adjust the pH of the electrolyte. To determine how effective, the composite electrodes were at removing phenol, initial experiments were carried out at 25 mA/cm^2, 1 g/l NaCl, and pH 3. The results are reported in Table 3.

Table 3. Phenol Removal Efficiency for Mn-Co Composite Oxide Prepared by Different Conditions

Conditions of prepared electrode	COD removal % at current density = 25 mA/cm^2, pH = 3, and NaCl conc. = 1 g/l	
	Anode	Cathode
Current density of 25 mA/cm^2	49.530	69.521
Current density of 30 mA/cm^2	37.391	55.891
Current density of 35 mA/cm^2	31.872	51.672

Therefore, the cathode prepared at 25 mA/cm^2 was the most effective electrode for COD elimination according to these results and the results of the characterization of the anode and cathode prepared with different current densities.

The optimal cathode electrode's performance is tested in a range of NaCl (1, 1.5, and 2 g/l), pH (3, 4, and 5), and current density (40, 60, and 80 mA/cm^2) to detect the effect of these conditions on the COD removal efficiency.

The removal efficiency of COD under different current densities (40, 60, and 80 mA/cm^2) was examined at NaCl = 1 g/l, and pH =3. As shown in Fig. 9, the removal efficiency increased as the current density increased due to the increase in the generation of HOCl. As the current density increases from 40 to 80 mA/cm^2, the removal percentage after 3 h of electrolysis increased from 79.224 to 96.656 %, respectively which is in agreement with previous studies [16, 48].

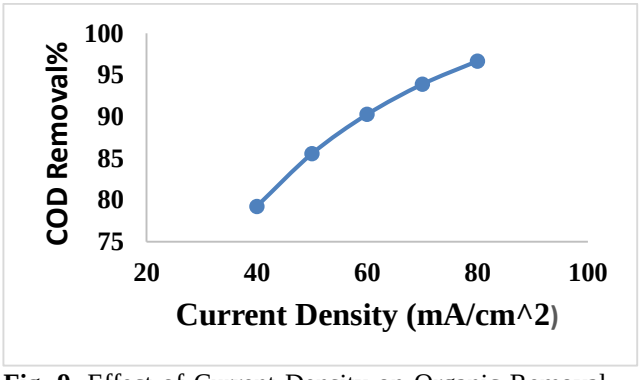

Fig. 9. Effect of Current Density on Organic Removal at NaCl = 1g/l, pH = 3, and time = 3h

Fig. 10 shows the removal efficiency of phenol under different values of pH, and the results showed that it

decreased from 96.656 to 88.84% as the pH value increased from 2 to 5, respectively, and this result agrees with previous work [16,48].

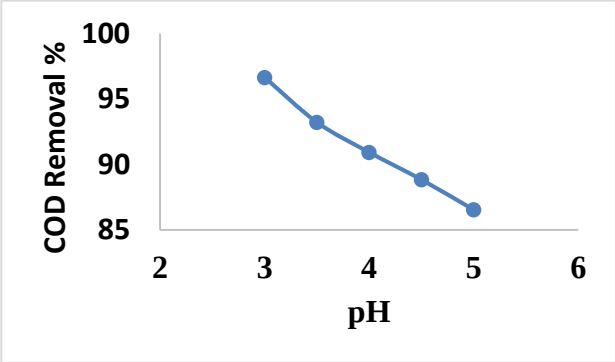

Fig. 10. Effect of pH on Organic Removal at Current Density 80 mA/cm^2, NaCl = 1g/l, and time = 3h

It must be established that the removal of phenol and any other by-products is attained by oxidation with reactive chlorine species such as chlorine (Cl_2), hypochlorous acid (HOCl), or hypochlorite ion (OCl^-). HOCl is the dominant oxidant which is more effective than other oxidants, so higher removal efficiencies are predicted at a more acidic medium. This can be expressed in Eq. 2 [49, 51, 52].

$$At\ anode: Cl_{2(diss.)} + H_2O \rightarrow H^+ + Cl^- + HOCl \quad (2)$$

Fig. 11 illustrates that due to the participation of active chlorine in the oxidation process, the efficiency with which COD is removed rises as the concentration of NaCl in the solution rises. The removal efficiency of COD increased slightly from 96.656 to 98.769 % when the concentration of NaCl in electrolyte increased from 1 to 2 g/l respectively, at 80 mA/cm^2, and pH= 3. The increase the concentration of NaCl leads to an increase in HOCl generation, which means higher removal efficiency and that agreed with previous studies [53, 2].

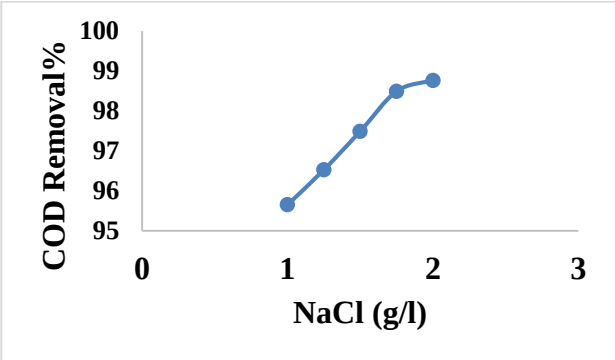

Fig. 11. Effect of NaCl on Organic Removal at Current Density 80 mA/cm^2, pH =3, and time = 3h

The current results showed that Mn-Co composite electrode is a very active electrode in eliminating phenol and any other by-products by reducing the required time for electrolysis to 3 h in comparison with previous studies that utilized other electrodes [54, 55, 56].

4- Conclusion

The Mn-Co composite electrode was prepared under different current densities by electrodeposition process. Based on the results of characterization, the composite electrodes of the metal oxides were prepared successfully anodically and cathodically. The optimum current density for electrodeposition of Mn-Co oxide was 25 mA/cm^2 according to the result of XRD, SEM, and AFM; hence, it gave good surface coverage with small roughness and with the highest value of COD removal.

Increasing the current density and the concentration of NaCl improved the effectiveness of removing phenol and its byproducts, whereas increasing the pH range in the electrolyte has the opposite effect. A high COD removal efficiency of 98.769 % was acquired in 3 h, which is considered an excellent result in comparison with previous studies that accomplished this removal with a longer electrolysis time.

Nomenclature

Nomenclature	**Meaning**	**Unit**
COD	Chemical Oxygen Demand	mg/l
COD_f	Final COD concentration	mg/l
COD_0	Initial COD concentration	mg/l
Symbol	**Definition**	
XRD	X-ray diffraction	
EDX	Energy-dispersive X-ray spectrometry	
SEM	scanning electronic microscopy	
$OH^•$	hydroxyl radical	
AFM	Atomic force microscopy	
RMS	Root mean square	
HOCl	hypochlorous acid	
OCl^-	hypochlorite ion	

References

[1] Z. I. Abbas and A. S. Abbas, "Optimization of the electro-fenton process for cod reduction from refinery wastewater," *Environ Eng Manag J*, vol. 19, no. 11, pp. 2029–2037, Oct. 2020, https://doi.org/10.30638/eemj.2020.192

[2] S. Chakawa and M. Aziz, "Investigating the result of current density, temperature, and electrolyte concentration on cod: Subtraction of petroleum refinery wastewater using response surface methodology," *Water (Switzerland)*, vol. 13, no. 6, Mar. 2021, https://doi.org/10.3390/w13060835

[3] A. D. M. de Medeiros, C. J. G. da Silva Junior, J. D. P. de Amorim, I. J. B. Durval, A. F. de Santana Costa, and L. A. Sarubbo, "Oily Wastewater Treatment: Methods, Challenges, and Trends," *Processes*, vol. 10, no. 4. MDPI, Apr. 01, 2022. https://doi.org/10.3390/pr10040743

[4] W. T. Mohammed, S. M. Abdullah, and A. M. Ghalib, "Catalytic Wet Air Oxidation of Phenol in a Trickle Bed Reactor," *Iraqi Journal of Chemical and Petroleum Engineering*, vol. 8, no. 4, pp. 45–52, 2007, https://doi.org/10.31699/IJCPE.2007.4.7

[5] N. Panigrahy, A. Priyadarshini, M. M. Sahoo, A. K. Verma, A. Daverey, and N. K. Sahoo, "A comprehensive review on eco-toxicity and biodegradation of phenolics: Recent progress and future outlook," *Environmental Technology and Innovation*, vol. 27. Elsevier B.V., Aug. 01, 2022. https://doi.org/10.1016/j.eti.2022.102423

[6] A. S. Abbas, M. H. Hafiz, and R. H. Salman, "Indirect Electrochemical Oxidation of Phenol Using Rotating Cylinder Reactor," *Iraqi Journal of Chemical and Petroleum Engineering*, vol. 17, no. 4, pp. 43–55, 2016, https://doi.org/10.31699/IJCPE.2016.4.5

[7] O. Al-Madanat, Y. Alsalka, W. Ramadan, and D. W. Bahnemann, "WTiO2 photocatalysis for the transformation of aromatic water pollutants into fuels," *Catalysts*, vol. 11, no. 3. MDPI, pp. 1–45, Mar. 01, 2021. https://doi.org/10.3390/catal11030317

[8] L. G. C. Villegas, N. Mashhadi, M. Chen, D. Mukherjee, K. E. Taylor, and N. Biswas, "A Short Review of Techniques for Phenol Removal from Wastewater," *Current Pollution Reports*, vol. 2, no. 3. Springer, pp. 157–167, Sep. 01, 2016. https://doi.org/10.1007/s40726-016-0035-3

[9] R. N. Abbas and A. S. Abbas, "Kinetics and Energetic Parameters Study of Phenol Removal from Aqueous Solution by Electro-Fenton Advanced Oxidation Using Modified Electrodes with PbO2 and Graphene," *Iraqi Journal of Chemical and Petroleum Engineering*, vol. 23, no. 2, pp. 1–8, Jun. 2022, https://doi.org/10.31699/ijcpe.2022.2.1

[10] E. M. Abou-Taleb, M. S. Hellal, and K. H. Kamal, "Electro-oxidation of phenol in petroleum wastewater using a novel pilot-scale electrochemical cell with graphite and stainless-steel electrodes," *Water and Environment Journal*, vol. 35, no. 1, pp. 259–268, Feb. 2021, https://doi.org/10.1111/wej.12624

[11] X. Sun, C. Wang, Y. Li, W. Wang, and J. Wei, "Treatment of phenolic wastewater by combined UF and NF/RO processes," *Desalination*, vol. 355, pp. 68–74, Jan. 2015, https://doi.org/10.1016/j.desal.2014.10.018

[12] H. M. Ibrahim and R. H. salman, "Study the Optimization of Petroleum Refinery Wastewater Treatment by Successive Electrocoagulation and Electro-oxidation Systems," *Iraqi Journal of Chemical and Petroleum Engineering*, vol. 23, no. 1, pp. 31–41, Mar. 2022, https://doi.org/10.31699/ijcpe.2022.1.5

[13] L. G. C. Villegas, N. Mashhadi, M. Chen, D. Mukherjee, K. E. Taylor, and N. Biswas, "A Short Review of Techniques for Phenol Removal from Wastewater," *Current Pollution Reports*, vol. 2, no. 3. Springer, pp. 157–167, Sep. 01, 2016. https://doi.org/10.1007/s40726-016-0035-3

[14] O. Garcia-Rodriguez, E. Mousset, H. Olvera-Vargas, and O. Lefebvre, "Electrochemical treatment of highly concentrated wastewater: A review of experimental and modeling approaches from lab-to full-scale," *Crit Rev Environ Sci Technol*, pp. 1–70, 2022, https://doi.org/10.1080/10643389.2020.1820428

[15] M. A. Zazouli and M. Taghavi, "Phenol Removal from Aqueous Solutions by Electrocoagulation Technology Using Iron Electrodes:Effect of Some Variables," *J Water Resour Prot*, vol. 04, no. 11, pp. 980–983, 2012, https://doi.org/10.4236/jwarp.2012.411113

[16] P. Kariyajjanavar, "Degradation of Textile Wastewater by Electrochemical Method," *Hydrol Current Res*, vol. 02, no. 01, 2011, https://doi.org/10.4172/2157-7587.1000110

[17] X. Y. Li, Y. H. Cui, Y. J. Feng, Z. M. Xie, and J. D. Gu, "Reaction pathways and mechanisms of the electrochemical degradation of phenol on different electrodes," *Water Res*, vol. 39, no. 10, pp. 1972–1981, 2005, https://doi.org/10.1016/j.watres.2005.02.021

[18] C. Zhang, Y. Jiang, Y. Li, Z. Hu, L. Zhou, and M. Zhou, "Three-dimensional electrochemical process for wastewater treatment: A general review," *Chemical Engineering Journal*, vol. 228, pp. 455–467, 2013, https://doi.org/10.1016/j.cej.2013.05.033

[19] C. A. Martínez-Huitle and M. Panizza, "Electrochemical oxidation of organic pollutants for wastewater treatment," *Current Opinion in Electrochemistry*, vol. 11. Elsevier B.V., pp. 62–71, Oct. 01, 2018. https://doi.org/10.1016/j.coelec.2018.07.010

[20] R. H. Salman and A. H. Abbar, "Optimization of a combined electrocoagulation-electro-oxidation process for the treatment of Al-Basra Majnoon Oil field wastewater: Adopting a new strategy," *Chemical Engineering and Processing - Process Intensification*, vol. 183, Jan. 2023, https://doi.org/10.1016/j.cep.2022.109227

[21] A. S. Mramba, P. P. Ndibewu, L. L. Sibali, and K. Makgopa, "A Review on Electrochemical Degradation and Biopolymer Adsorption Treatments for Toxic Compounds in Pharmaceutical Effluents," *Electroanalysis*, vol. 32, no. 12. Wiley-VCH Verlag, pp. 2615–2634, Dec. 01, 2020. https://doi.org/10.1002/elan.202060454

[22] G. Naser, T. Mohammed, and A. Abbar, "A novel Tubular Electrochemical Reactor with a Spiral Design of Anode for Treatment of Petroleum Refinery Wastewater," *Egypt J Chem*, vol. 66, no. 1, pp. 257–270, 2023, https://doi.org/10.21608/ejchem.2022.125257.5574

[23] A. N. Kassob and A. H. Abbar, "Treatment of Petroleum Refinery Wastewater by Graphite–Graphite Electro Fenton System Using Batch Recirculation Electrochemical Reactor," *Journal of Ecological Engineering*, vol. 23, no. 10, pp. 291–303, 2022, https://doi.org/10.12911/22998993/152524

[24] Y. Jiang *et al.*, "Anodic oxidation for the degradation of organic pollutants: Anode materials, operating conditions and mechanisms. A mini review," *Electrochemistry Communications*, vol. 123. Elsevier Inc., Feb. 01, 2021. https://doi.org/10.1016/j.elecom.2020.106912

[25] D. Rajkumar, J. G. Kim, and K. Palanivelu, "Indirect electrochemical oxidation of phenol in the presence of chloride for wastewater treatment," *Chem Eng Technol*, vol. 28, no. 1, pp. 98–105, 2005, https://doi.org/10.1002/ceat.200407002

[26] M. Panizza and G. Cerisola, "Direct and Mediated Anodic Oxidation of Organic Pollutants," *Chem Rev*, vol. 109, no. 12, pp. 6541–6569, 2009, https://doi.org/10.1021/cr9001319

[27] Adel M. A. Mohamed and Teresa D. Golden, *Electrodeposition of Composite Materials.*, First published. ExLi4EvA, 2016. https://doi.org/10.5772/60892

[28] M. Foroughi *et al.*, "Electrodegradation of tetracycline using stainless steel net electrodes: Screening of main effective parameters and interactions by means of a two-level factorial design," *Korean Journal of Chemical Engineering*, vol. 34, no. 11, pp. 2999–3008, Nov. 2017, https://doi.org/10.1007/s11814-017-0212-0

[29] R. H. Salman, M. H. Hafiz, and A. S. Abbas, "The performance of MnO2/graphite electrode for TOC removal from wastewater by indirect electrochemical oxidation process," in *IOP Conference Series: Materials Science and Engineering*, Institute of Physics Publishing, Dec. 2018. https://doi.org/10.1088/1757-899X/454/1/012148

[30] O. Scialdone, S. Randazzo, A. Galia, and G. Silvestri, "Electrochemical oxidation of organics in water: Role of operative parameters in the absence and in the presence of NaCl," *Water Res*, vol. 43, no. 8, pp. 2260–2272, 2009, https://doi.org/10.1016/j.watres.2009.02.014

[31] and I. O. Anglada, Ane Urtiaga, "Contributions of electrochemical oxidation to waste-water treatment: fundamentals," *J Chem Technol Biotechnol*, vol. 84, no. April, pp. 1747–1755, 2009, https://doi.org/10.1002/jctb.2214

[32] H. M. Lee, K. Lee, and C. K. Kim, "Electrodeposition of manganese-nickel oxide films on a graphite sheet for electrochemical capacitor applications," *Materials*, vol. 7, no. 1, pp. 265–274, 2014, https://doi.org/10.3390/ma7010265

[33] R. H. Salman, M. H. Hafiz, and A. S. Abbas, "Preparation and Characterization of Graphite Substrate Manganese Dioxide Electrode for Indirect Electrochemical Removal of Phenol," *Russian Journal of Electrochemistry*, vol. 55, no. 5, pp. 407–418, May 2019, https://doi.org/10.1134/S1023193519050124

[34] J. T. Hasan and R. H. Salman, "Electrosorption of cadmium ions from the aqueous solution by a MnO2/carbon fiber composite electrode," *Desalination Water Treat*, vol. 243, pp. 187–199, Dec. 2021, https://doi.org/10.5004/dwt.2021.27885

[35] Yamama A. Ahmed, Rasha H. Salman, Simultaneous electrodeposition of multicomponent of Mn– Co–Ni oxides electrodes for phenol removal by anodic oxidation, Case Studies in Chemical and Environmental Engineering, Volume 8, 2023, https://doi.org/10.1016/j.cscee.2023.100386

[36] K. Cysewska *et al.*, "The influence of the electrodeposition parameters on the properties of Mn-Co-based nanofilms as anode materials for alkaline electrolysers," *Materials*, vol. 13, no. 11, Jun. 2020, https://doi.org/10.3390/ma13112662

[37] S. L. Kadam, S. M. Mane, P. M. Tirmali, and S. B. Kulkarni, "Electrochemical synthesis of flower like Mn-Co mixed metal oxides as electrode material for supercapacitor application," *Current Applied Physics*, vol. 18, no. 4, pp. 397–404, Apr. 2018, https://doi.org/10.1016/j.cap.2018.01.019

[38] J. K. Chang, M. T. Lee, C. H. Huang, and W. T. Tsai, "Physicochemical properties and electrochemical behavior of binary manganese-cobalt oxide electrodes for supercapacitor applications," *Mater Chem Phys*, vol. 108, no. 1, pp. 124–131, Mar. 2008, https://doi.org/10.1016/j.matchemphys.2007.09.013

[39] E. M. Abebe and M. Ujihara, "Simultaneous Electrodeposition of Ternary Metal Oxide Nanocomposites for High-Efficiency Supercapacitor Applications," *ACS Omega*, vol. 7, no. 20, pp. 17161–17174, May 2022, https://doi.org/10.1021/acsomega.2c00826

[40] P. Daniel Nixon and C. Joseph Kennady, "Electrodeposition of manganese-nickel oxide films for supercapacitor applications," *Voprosy Khimii i Khimicheskoi Tekhnologii*, vol. 2019, no. 6, pp. 144–148, 2019, https://doi.org/10.32434/0321-4095-2019-127-6-144-148

[41] E. Moti', M. H. Shariat, and M. E. Bahrololoom, "Influence of cathodic overpotential on grain size in nanocrystalline nickel deposition on rotating cylinder electrodes," *J Appl Electrochem*, vol. 38, no. 5, pp. 605–612, May 2008, https://doi.org/10.1007/s10800-007-9478-y

[42] A. M. Rashidi and A. Amadeh, "The effect of current density on the grain size of electrodeposited nanocrystalline nickel coatings," *Surf Coat Technol*, vol. 202, no. 16, pp. 3772–3776, May 2008, https://doi.org/10.1016/j.surfcoat.2008.01.018

[43] H. Zhu, S. Geng, G. Chen, and F. Wang, "Effect of Current Density on Deposition of Ni-Mn 3 O 4 Composite Coating and its High Temperature Behavior," *J Electrochem Soc*, vol. 167, no. 4, p. 041506, Feb. 2020, https://doi.org/10.1149/1945-7111/ab754c

[44] H. T. Yang *et al.*, "Effects of current density on preparation and performance of Al/conductive coating/α-PbO2-CeO2-TiO2/β-PbO2-MnO2-WC-ZrO2 composite electrode materials," *Transactions of Nonferrous Metals Society of China (English Edition)*, vol. 24, no. 10, pp. 3394–3404, 2014, https://doi.org/10.1016/S1003-6326(14)63482-8

[45] A. Kassim, S. Nagalingam, H. S. Min, and N. Karrim, "XRD and AFM studies of ZnS thin films produced by electrodeposition method," *Arabian Journal of Chemistry*, vol. 3, no. 4, pp. 243–249, Oct. 2010, https://doi.org/10.1016/j.arabjc.2010.05.002

[46] D. G. Foster, Y. Shapir, and J. Jorne, "The Effect of Rate of Surface Growth on Roughness Scaling," *J Electrochem Soc*, vol. 152, no. 7, p. C462, 2005, https://doi.org/10.1149/1.1921767

[47] L. Liu., and X. Zhu., "Influence of Current Density on Orientation-Controllable Growth and Characteristics of Electrochemically Deposited Au Films," *J Electrochem Soc*, vol. 166, no. 1, pp. D3232–D3237, 2019, https://doi.org/10.1149/2.0291901jes

[48] E. M. Abou-Taleb, M. S. Hellal, and K. H. Kamal, "Electro-oxidation of phenol in petroleum wastewater using a novel pilot-scale electrochemical cell with graphite and stainless-steel electrodes," *Water and Environment Journal*, vol. 35, no. 1, pp. 259–268, Feb. 2021, https://doi.org/10.1111/wej.12624

[49] K. Zhu, H. Qi, X. Sun, and Z. Sun, "Anodic oxidation of diuron using Co 3 O 4 /graphite composite electrode at low applied current," *Electrochim Acta*, vol. 299, pp. 853–862, Mar. 2019, https://doi.org/10.1016/j.electacta.2019.01.072

[50] K. Rajkumar and M. Muthukumar, "Response surface optimization of electro-oxidation process for the treatment of C.I. Reactive Yellow 186 dye: reaction pathways," *Appl Water Sci*, vol. 7, no. 2, pp. 637–652, May 2017, https://doi.org/10.1007/s13201-015-0276-0

[51] J. de J. Treviño-Reséndez, A. Medel, and Y. Meas, "Electrochemical technologies for treating petroleum industry wastewater," *Current Opinion in Electrochemistry*, vol. 27. Elsevier B.V., Jun. 01, 2021. https://doi.org/10.1016/j.coelec.2021.100690

[52] J. P. de P. Barreto, E. V. dos Santos, M. M. Oliveira, D. R. da Silva, J. F. de Souza, and C. A. Martínez-Huitle, "Electrochemical mediated oxidation of phenol using Ti/IrO2 and Ti/Pt-SnO2-Sb2O5 electrodes," *Journal of Electrochemical Science and Engineering*, vol. 4, no. 4, pp. 259–270, Dec. 2014, https://doi.org/10.5599/jese.2014.0069

[53] D. Rajkumar, J. G. Kim, and K. Palanivelu, "Indirect electrochemical oxidation of phenol in the presence of chloride for wastewater treatment," *Chem Eng Technol*, vol. 28, no. 1, pp. 98–105, Jan. 2005, https://doi.org/10.1002/ceat.200407002

[54] R. H. Salman, M. H. Hafiz, and A. S. Abbas, "Preparation and Characterization of Graphite Substrate Manganese Dioxide Electrode for Indirect Electrochemical Removal of Phenol," *Russian Journal of Electrochemistry*, vol. 55, no. 5, pp. 407–418, May 2019, https://doi.org/10.1134/S1023193519050124

[55] R. N. Abbas and A. S. Abbas, "The Taguchi Approach in Studying and Optimizing the Electro-Fenton Oxidation to Reduce Organic Contaminants in Refinery Wastewater Using Novel Electrodes," *Technology & Applied Science Research*, vol. 12, no. 4, pp. 8928–8935, 2022, https://doi.org/10.48084/etasr.5091

[56] R. Berenguer, T. Valdés-Solís, A. B. Fuertes, C. Quijada, and E. Morallón, "Cyanide and Phenol Oxidation on Nanostructured Co[sub 3]O[sub 4] Electrodes Prepared by Different Methods," *J Electrochem Soc*, vol. 155, no. 7, p. K110, 2008, https://doi.org/10.1149/1.2917210

التحضير الأنودي والكاثودي لأنودات القطب المركب MnO_2 / Co_2O_3 للأكسدة الكهربائية للفينول

يمامة عبد الكريم احمد [١]، رشا حبيب سلمان [١]، فاطمة كانديمرلي [٢،*]

١ قسم الهندسة الكيمياوية، كلية الهندسة، جامعة بغداد، بغداد، العراق
٢ جامعه قسطمونة، كلية الهندسة والاعمار، قسم هندسة الطب الحياتي، تركيا

الخلاصة

مادة الأنود الاقتصادية وذات الأداء العالي هي العامل الحاسم الذي يؤثر على كفاءة الأكسدة الكهربائية للمواد العضوية. هدفت الدراسة الحالية إلى الكشف عن أفضل الظروف لتحضير مركب أوكسيد Mn–Co والذي سيكون بمثابة الأنودات في نظام الأكسدة الكهربائية للفينول. يتم تحضير الأنودات المركبة بنجاح بثبوت التيار بواسطة الترسيب الأنودي والكاثودي. تم فحص التركيب والحجم البلوري للقطب المركب لأوكسيد Mn–Co باستخدام مقياس حيود الأشعة السينية (XRD)، ودُرست الخصائص المورفولوجية للإلكترود المُعد عن طريق المسح المجهري الإلكتروني (SEM) ومجهر القوة الذرية (AFM)، والتركيب الكيميائي للأوكسيد المترسب المختلف تم تقديره بواسطة التحليل الطيفي للأشعة السينية المشتتة للطاقة (EDX). تم فحص ترسيب أوكسيد Mn–Co على ركيزة الجرافيت عند ٢٥ و ٣٠ و ٣٥ مللي أمبير/ سم^{٢} للكشف عن أفضل الظروف للترسيب. أعطت الكثافة الحالية ٢٥ مللي أمبير/سم^{٢} أفضل ترسيب كاثودي. تأثير كثافة التيار (٤٠ و ٦٠ و ٨٠ مللي أمبير/سم^{٢}) ودرجة الحموضة (٣ و ٤ و ٥) وتركيز كلوريد الصوديوم (١، ١,٥، و ٢ جم/لتر) على الأكسدة الكهربائية الأنودية للفينول وتم قياس الحاجة الكيميائية للأوكسجين (COD) لكل تجربة إزالة. زادت كفاءة إزالة الفينول والمنتجات الثانوية الأخرى مع زيادة كثافة التيار وتركيز كلوريد الصوديوم في الإلكتروليت، بينما انخفضت مع زيادة الرقم الهيدروجيني. أعطى القطب المركب المحضر كفاءة إزالة عالية لـ COD وصلت الى ٩٨,٧٦٩% عند كثافة تيار ٨٠ مللي أمبير/سم^{٢}، pH = 3، و تركيز كلوريد الصوديوم = ٢ جم/لتر خلال ٣ ساعات.

الكلمات الدالة: أوكسيد المنغنيز، أوكسيد الكوبالت، الفينول، القطب المركب، الترسيب الكهربائي، الأكسدة الكهربائية.